Available online at www.sciencedirect.com
ScienceDirect
Journal of Organometallic Chemistry 692 (2007) 4519–4527
Journal of Organometallic Chemistry
www.elsevier.com/locate/jorganchem

Regiochemistry of propene insertion with group 4 polymerization catalysts from a theoretical perspective

Andrea Correa [a], Giovanni Talarico [b], Luigi Cavallo [a,*]

[a] *Dipartimento di Chimica, Università di Salerno – Via Ponte don Melillo, I-84084 Fisciano (SA), Italy*
[b] *Dipartimento di Chimica, Università di Napoli – Via Cintia, I-80100 Napoli, Italy*

Received 14 February 2007; received in revised form 11 April 2007; accepted 11 April 2007
Available online 21 April 2007

Abstract

The regiochemistry of monomer insertion in propene polymerization promoted by group 4 metal catalysts has been investigated by using DFT methods. We calculated primary and secondary propene insertion on metallocenes, constrained geometry catalysts and post-metallocene systems analyzing the effects of ligand framework, growing chain and metal. Our study supports the concept that for metallocene-based catalysts the regiochemistry of propene is mainly originated by steric effects. Instead, for octahedral systems a delicate balance between steric and electronic effects is found. This allows to play with the electronic properties of the ligand framework to tune finely the regiochemistry of polymerization.

Keywords: Propene polymerization; Regiochemistry; DFT calculations

1. Introduction

It is commonly referred in literature that propene enchainment into M–C bonds promoted by catalysts based on early transition metals occurs predominantly through primary (or 1,2) insertion (see Scheme 1) [1]. Secondary (or 2,1) propene insertion, commonly referred to as regio-irregular insertion or regiomistake, is a sporadic event which usually corresponds to less than 1% of the enchainments [2].

This basic concept holds for the classical heterogeneous catalysts based on $TiCl_3$ or $TiCl_4$ supported on $MgCl_2$ [1], as well as for the homogeneous group 4 metallocene systems [3] and the so-called constrained geometry catalyst (CGC) formed by a linked (amido-cyclopentadienyl) ligand [4]. The fact that the recently discovered octahedral C_2-symmetric phenoxy-amine Zr complexes [5] or trigonal-bipyramidal C_1 symmetric pyridyl-amine Hf systems [6] promote primary polymerization of various α-olefins regioselectively, seemed simply an extension to this well-accepted fact.

Despite the clear preference for primary enchainment shown by an overwhelming number of catalysts, secondary propene insertion into the M–alkyl bond is known since the 1960s, when homogenous V-based catalytic systems were shown to promote syndiotactic propene polymerization through prevailingly secondary enchainments [7]. These systems were probably considered the exception that confirmed the rule. However, the recent discovery that well-defined homogeneous bis(phenoxy-imine)$TiCl_2$ precursors, despite the strong similarity with the tetradentate bis(phenoxy-amine) analogs, promote syndiotactic propene polymerization through secondary monomer insertion [8] opened new questions. It appears that secondary enchainments might be not only sporadic events, but can have a strong influence on the stereospecificity of the polymerization process.

In addition, it is worthy to recall that the regiodefects produced by an occasional 2,1 insertion during primary propagation have a strong effect on the materials properties

* Corresponding author.
E-mail address: lcavallo@unisa.it (L. Cavallo).

0022-328X/$ - see front matter © 2007 Elsevier B.V. All rights reserved.
doi:10.1016/j.jorganchem.2007.04.015

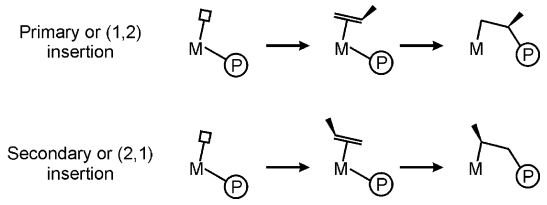

Scheme 1.

(e.g. lowering crystallinity and melting point of stereoregular polypropylenes) [9]. At the same time, there is also a close correlation between catalyst regioselectivity on one side and catalyst activity and polymer molecular mass on the other, due to the lower monomer insertion rate at a secondary growing chain end, and the competing β-H transfer to the monomer after a secondary insertion [3].

For these reasons, a rationalization of the factors that control regioirregular insertion is of relevance, and several theoretical studies already addressed this point. Molecular mechanics calculations on models of tetrahedral metallocene-based catalysts have clearly indicated that 2,1 propene insertion is disfavored by steric interactions between the propene methyl group and the metallocene skeleton, and that suitable substitution of the ligand can either reduce or increase the amount of secondary insertions [10]. On the other hand, we also suggested that electronic effects have a role, and that the different behavior of the post-metallocene bis(phenoxy-imine) and bis(phenoxy-amine) systems is the result of a delicate balance between (expected) steric and (unexpected) electronic effects. In particular, we suggested that higher electron density at the metal (i.e. in the presence of an electron-donating sp^3 amine N atom) favors primary propene insertion, whereas reduced electron density at the metal (i.e. in the presence of the less electron-donating sp^2 imine N atom) makes secondary insertion far more likely [11]. This trans effect is due to destabilizing interaction between electron density at the metal atom with electron density at the C atom that will form the new M–C bond. When propene is polymerized this destabilizing interaction is stronger in the case of secondary insertion because the secondary carbon atom of propene carries more electron density relative to the primary carbon atom, due to the inductive effect of the Me group [12].

The above mentioned studies focused on selected catalysts and a systematic comparison of the regiochemistry promoted by different ligand frameworks has never been performed. In this manuscript we try to fulfill this lack. To this end, we report here a systematic study of steric and electronic effects on the regioselectivity of 1-alkene insertion promoted by catalysts with pseudo-tetrahedral (e.g. metallocenes and CGC) and with octahedral geometry of coordination. For each class of systems we analyzed the effect on regiochemistry of different bulky ligands, growing chains, metals and different monomers insertion. The full list of the catalyst precursors investigated is reported in Chart 1.

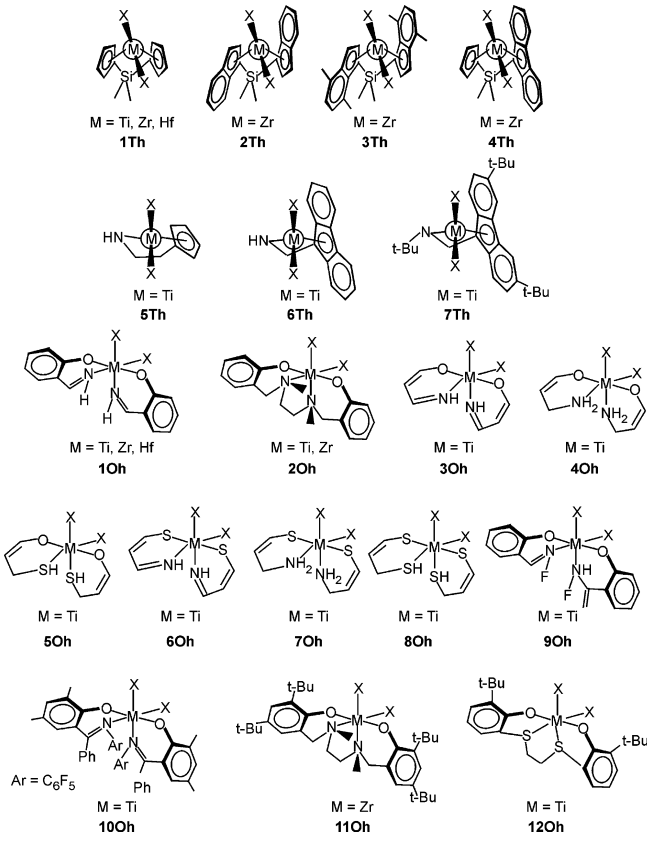

Chart 1.

More in depth, for metallocene systems we selected: the aspecific C_{2V}-symmetric $Me_2Si(Cp)_2MCl_2$ catalyst (M = Ti, Zr, Hf), (**1Th**), the isospecific C_2-symmetric, $Me_2Si(1\text{-Ind})_2ZrCl_2$ (**2Th**) and $Me_2Si(4,7\text{-Me}_2\text{-1-Ind})_2ZrCl_2$ (**3Th**) catalysts, and the syndiospecific C_s-symmetric $Me_2Si(Cp)(9\text{-Flu})ZrCl_2$ catalyst, (**4Th**); whereas for the CGC precursors we considered the $CpCH_2CH_2(N\text{-}^tBu)ZrCl_2$ (**5Th**), the $[Me_2Si(9\text{-Flu})(NH)]TiCl_2$ (**6Th**) and the syndiospecific $[Me_2Si(3,6\text{-}^tBu_2\text{-9-Flu})(N\text{-}^tBu)]TiCl_2$ (**7Th**) systems, where Me, Cp, Ind and Flu indicate methyl group, cyclopentadienyl, indenyl and fluorenyl ligands, respectively.

For octahedral non-metallocene systems we considered models of syndiospecific bis(phenoxy-imine) based catalysts (**1Oh**) (M = Ti, Zr, Hf) and of the isospecific bis(phenoxy-amine) based catalysts (**2Oh**) (M = Ti, Zr). In order to evaluate the ligand effects on insertion's regiochemistry the model systems **3Oh-8Oh** were also considered. System **9Oh** has been considered since it is a C_1-symmetric catalyst bearing an imine and an amine N atom. Finally, systems **10Oh-12Oh** are representative cases of real systems.

2. Computational details

Stationary points on the potential energy surface were calculated with the Amsterdam Density Functional (ADF) program system [13], developed by Baerends et al. [14]. The electronic configuration of the molecular systems were described by a triple-ζ STO basis set on Ti for 3s, 3p,

3d, 4s, 4p, on Zr for 4s, 4p, 4d, 5s, 5p, and on Hf for 5s, 5p, 5d, 6s, 6p (ADF basis set TZP). Double-ζ STO basis sets were used for S (3s, 3p), F, O, N and C (2s, 2p) and H (1s), augmented with a single 3d, 3d, and 2p function, respectively (ADF basis set DZP). The inner shells on Ti and S (including 2p), Zr (3d), Hf (4f) F, O, N and C (1s), were treated within the frozen core approximation. Energies and geometries were evaluated by using the local exchange-correlation potential by Vosko et al. [15], augmented in a self-consistent manner with Becke's exchange gradient correction [16] and Perdew's correlation gradient correction [17].

The regioselectivity of each system, $\Delta E^{\neq}_{regio}$, was calculated as the energy difference between the transition states leading to secondary and primary insertion of the monomer. Within this choice, positive values of $\Delta E^{\neq}_{regio}$ means that primary insertion is favored.

3. Results and discussion

For the sake of readability, we separated this section in two parts: the first is devoted to the analysis of the steric and electronic effects on the regioselectivity of 1-alkene insertion with metallocene and CGC systems; in the second part the same approach has been applied to the non-metallocene systems. Each section has been split in four sub-paragraph in which the: (a) *ligand effect*; (b) *growing chain effect*; (c) *metal effect* and (d) *monomer effect*, have been analyzed separately. Note that for the CGC systems we have also considered the role of the counterion on the regiochemistry of propene insertion.

3.1. Metallocene and CGC systems

The $\Delta E^{\neq}_{regio}$ and some geometrical parameters we calculated for the metallocene and the CGC systems of Chart 1 are reported in Table 1.

3.1.1. Metallocene and CGC systems: ligand effect

To address this point, we calculated the $\Delta E^{\neq}_{regio}$ for propene insertion into the Zr-^{i}Bu bond promoted by the metallocenes **1Th-Zr**, **2Th-Zr**, **3Th-Zr** and **4Th-Zr**, of Chart 1. The transition states we obtained correspond to the classical Cossee-like four-centers geometries and are stabilized by a strong α-agostic interaction. These geometries are very similar to those reported in previous papers on ethene and propene insertion with other group 4 polymerization catalysts [3]. As example we report those for **2Th-Zr** and **4Th-Zr**, (see Fig. 1). The length of the breaking Zr–C1 bond (see Fig. 1 for labels), as well as that of the emerging C1–C2 bond, are rather similar in all the transition states whereas the forming Zr–C3 bond is considerably longer in the transition states for secondary propene insertion (see Table 1). In all the cases, the growing chain is placed in an open part of space to reduce steric interactions with the ligand. For the isospecific **2Th-Zr** system (see Fig. 1), and similarly for the syndiospecific **4Th-Zr** system, this means that the growing chain develops away from the nearby six-membered aromatic ring of the ligand, in agreement with the mechanism of the chiral orientation of the growing chain [18]. Additionally, in the case of primary propene insertion the methyl group of the propene is oriented anti to (i.e. away from) the growing chain for all the systems. Differently, in the case of secondary propene insertion the orientation of the methyl group of the monomer is not dependent on the position of the growing chain. Instead, it is oriented in such a way to minimize steric interactions with the ligand. This means that the methyl group of the secondary inserting propene is away from the nearby six-membered ring of the ligand in **2Th-Zr** and **4Th-Zr**. These features, which minimize steric interactions between different groups, were shown to be at the origin of the stereoselectivity in both primary and secondary insertion [18].

The $\Delta E^{\neq}_{regio}$ values reported in Table 1 for the **1Th-Zr**, **2Th-Zr** and **4Th-Zr** metallocenes, (about 2.5 kcal/mol), show that primary insertion is always favored. The $\Delta E^{\neq}_{regio}$ are rather similar to the molecular mechanics (MM) $\Delta E^{\neq}_{regio}$ previously reported by Guerra and coworkers [10c,10d]. Considering that MM calculations only include steric interactions, the similarity between the QM and MM $\Delta E^{\neq}_{regio}$ values clearly indicates that the driving force for primary propene insertion with metallocene-based catalysts is steric in nature. As already indicated, the preference for primary insertion can be ascribed to steric interactions between the methyl group of the secondary inserting propene and the ligand framework. Nevertheless, steric effects can be also used to increase the amount of regioirregularities. For example, in line with experimental results and previous MM calculations [10e], the $\Delta E^{\neq}_{regio}$ for the **3Th-Zr** is considerably reduced, due to steric interactions between the methyl group of the primary inserting propene with the methyl group in position 4 of the bis-indenyl skeleton of **3Th-Zr**.

As regards the stereoselectivity of secondary propene insertion, the numbers reported in Table 1 clearly indicate that secondary insertion is remarkably enantioselective with both the iso- and syndiospecific **2Th-Zr** and **4Th-Zr** systems, while it is scarcely enantioselective in the case of the aspecific **1Th-Zr** system. Moreover, they also evidence a remarkable difference between the isospecific and syndiospecific model complexes, related to the chirality of the inserting propene molecule. In fact, in line with previous studies [10c,10d], for the isospecific system secondary and primary propene insertions correspond to opposite chiralities of coordination of the monomer, whereas for the syndiospecific system they correspond to the same chirality of coordination of the monomer, (see Fig. 1). The picture is consistent also if the CGC systems **5**–**7Th-Ti** are considered. Small amido substituents and larger bridge (e.g. CH_2CH_2) decrease $\Delta E^{\neq}_{regio}$, (see **5Th-Ti** and **6Th-Ti** $\Delta E^{\neq}_{regio}$ values). However, as soon as bulky substituents are introduced on the amido group (**7Th-Ti**), the $\Delta E^{\neq}_{regio}$ increases again reaching a value similar to that calculated for the metallocene systems. This finding is in line with the

Table 1
Energy differences, $\Delta E^{\ddagger}_{regio}$, between the transition states for 2,1 and 1,2 propene insertion, and some geometrical parameters (see Fig. 1 for the labeling scheme) for metallocene and CGC systems of Chart 1

Model	Alkyl	$\Delta E^{\ddagger}_{regio}$ (kcal/mol)	Insertion	M–C1 (Å)	M–C3 (Å)	C1–C2 (Å)
1Th-Ti	^{i}Bu	2.9	1,2	2.23	2.28	2.20
			2,1	2.18	2.45	2.24
1Th-Zr	Me	3.9	1,2	2.33	2.37	2.15
			2,1	2.32	2.44	2.13
1Th-Zr	Et	3.3	1,2	2.35	2.37	2.19
			2,1	2.34	2.45	2.17
1Th-Zr	^{i}Bu	2.6 (3.5)[a]	1,2	2.36	2.36	2.20
			2,1	2.33	2.46	2.20
1Th-Zr	^{i}Pr	0.9	1,2	2.42	2.35	2.23
			2,1	2.40	2.45	2.21
1Th-Hf	^{i}Bu	2.6	1,2	2.36	2.37	2.20
			2,1	2.33	2.46	2.20
2Th-Zr	^{i}Bu	2.5 (9.1)[a]	1,2	2.34	2.36	2.26
			2,1	2.34	2.44	2.26
3Th-Zr	^{i}Bu	1.6	1,2	2.36	2.36	2.27
			2,1	2.34	2.45	2.26
4Th-Zr	^{i}Bu	2.6 (8.4)[a]	1,2	2.35	2.36	2.27
			2,1	2.33	2.42	2.25
5Th-Ti	^{i}Bu	1.0	1,2	2.18	2.21	2.22
			2,1	2.14	2.30	2.19
5Th-Ti + (**Borate**)	^{i}Bu	1.0	1,2	2.15	2.26	2.31
			2,1	2.13	2.38	2.32
6Th-Ti	^{i}Bu	1.4	1,2	2.16	2.18	2.25
			2,1	2.14	2.10	2.22
7Th-Ti	^{i}Bu	3.1 (8.3)[a]	1,2	2.15	2.20	2.32
			2,1	2.14	2.26	2.25

[a] $\Delta E^{\neq}_{regio}$ of the "wrong" enantioface.

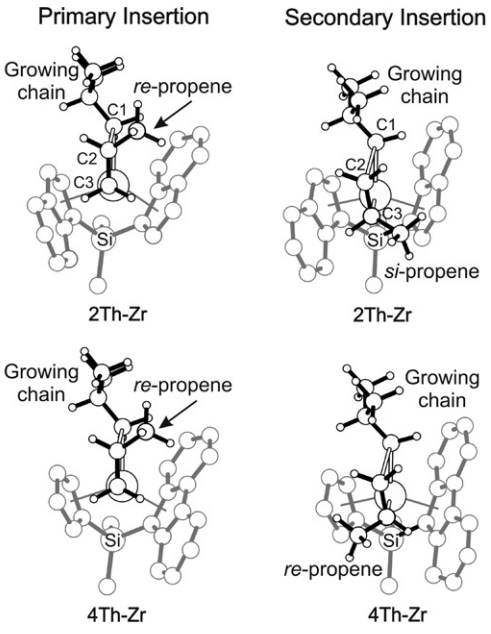

Fig. 1. Transition states for primary and secondary insertion into the M–^{i}Bu bond of the **2Th-Zr** and **4Th-Zr** metallocene catalysts of Chart 1.

experimental results, which indicated that the amount of regiomistakes depends of the bulkyness of the *N*-amido substituents [4].

3.1.2. Metallocene systems: growing chain effect

To understand the effect of the growing chain we calculated the $\Delta E^{\neq}_{regio}$ for propene insertion into the Zr–R bond (R = Me, Et, ^{i}Pr and ^{i}Bu) of the **1Th-Zr** system of Chart 1. It is worth noting that: (i) R = Me correspond to the alkyl group which is bonded to Zr in the initiation step; (ii) R = Et is the model for the growing chain bonded to Zr after a termination step (e.g. β-H transfer to the monomer or to the metal), or after ethene insertion in ethene/propene copolymerization; (iii) R = ^{i}Pr and ^{i}Bu are models of secondary and primary growing chains, respectively, in the case of propene homopolymerization. The $\Delta E^{\neq}_{regio}$ reported in Table 1 for propene insertion into the Zr–Me or Zr–Et bond is substantially the same, and it is roughly 1 kcal/mol higher than the $\Delta E^{\neq}_{regio}$ for insertion into the Zr–^{i}Bu bond, and roughly 3 kcal/mol higher that the $\Delta E^{\neq}_{regio}$ for insertion into the Zr–^{i}Pr bond. These numbers clearly indicate that the bulkiness of the growing chain has a strong effect on the regioselectivity of propene inser-

tion, and that in propene homopolymerization the regioselectivity in the initiation step as well as in the reactivation after a transfer reaction, is higher than during propagation. Moreover, in the case of ethene/propene copolymerization propene insertion after ethene is more regioselective than propene insertion after another propene molecule. This behavior can be mainly ascribed to steric interactions between the chain and the methyl group of the primary inserting propene. Some of these interactions are already present in the case of insertion into the Zr–^{i}Bu bond, and are much more relevant for propene insertion into the Zr–^{i}Pr bond (see Fig. 2). These conclusions are general, since are consequence of direct interaction between the monomer and the chain, and are independent of the ligand framework. This suggests that: (a) after a regiomistake (i.e.: in presence of a M-secondary chain bond) the regioselectivity of propene insertion is severely shifted toward secondary insertion; (b) in the initiation step and after termination by trans alkylation with $AlMe_3$, primary insertion is more favored that in the propagation step; (c) propene insertion after an ethene insertion, is more regioselective than the propene/propene homopolymerization step.

3.1.3. Metallocene systems: metal effect

To investigate the effect of the metal atom we compared the $\Delta E^{\neq}_{regio}$ for propene insertion into the M–^{i}Bu bond of the **1Th-M** metallocene of Chart 1 (M = Ti, Zr, Hf). For **1Th-Ti** we calculated a $\Delta E^{\neq}_{regio} = 2.9$ kcal/mol and a short Ti–C distance was observed (i.e. Ti–C3 = 2.28 Å); for **1Th-Zr** and **1Th-Hf** systems we found a lower regioselectivity ($\Delta E^{\neq}_{regio}$ about 2.6 kcal/mol for both of them) and an increase of 0.11 Å of the M–C distance with respect to the **1Th-Ti** system. The plot of Fig. 3 illustrates a clear relationship between the calculated $\Delta E^{\neq}_{regio}$ and the ionic radius of the metal. Specifically, $\Delta E^{\neq}_{regio}$ decreases with an increase of the ionic radius. Larger ionic radius results in longer M–C distances (see Table 1), which stabilizes the transition state for secondary propene insertion.

In agreement with the conclusions of the previous sections, this finding further supports the concept that the regioselectivity promoted by metallocenes is strongly dominated by steric effects, and that the methyl group of the secondary inserting propene cannot be accommodated easily in the compact reactive pocket shaped by the Cp rings.

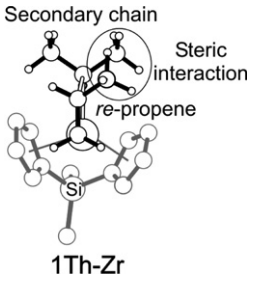

Fig. 2. Transition state for primary insertion into the M–^{i}Pr bond of the **1Th-Zr** catalyst of Chart 1.

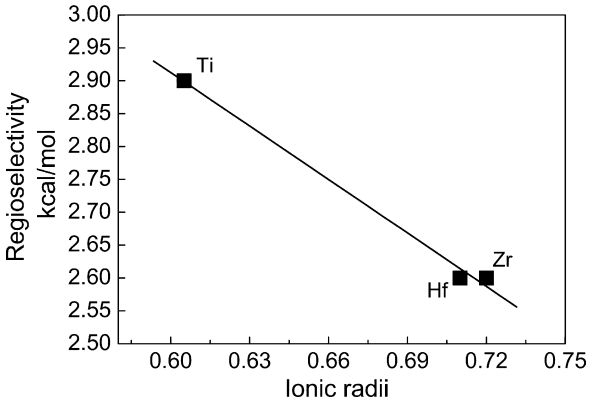

Fig. 3. Plot of the $\Delta E^{\neq}_{regio}$ vs. the ionic metal radius for propene insertion into the M–^{i}Bu bond of the **1Th-M** metallocene of Chart 1.

3.1.4. Metallocene systems: monomer effect

To investigate the influence of the monomer R group we compared the $\Delta E^{\neq}_{regio}$ calculated for insertion of different alkenes into the Zr–Me bond of system **1Th**. We replaced the methyl group of propene with more or less electron-donating substituents R (R = OCH_3, Cl, Ph, NO_2). Following ideas in the context of quantitative structure-properties relationship (QSPR), we report the $\Delta E^{\neq}_{regio}$ as function of the Hammet σ constant of the R group of the 1-alkene. The only scope of considering alkenes with R = OCH_3 and NO_2, which cannot be polymerized with these systems, is to have a set of monomers than span extremely different electronic properties, and to extract clear trends from such extremes.

The plot of Fig. 4 shows an almost linear trend of $\Delta E^{\neq}_{regio}$ with the Hammet σ constant, and that electron-donating groups reinforce primary insertion; mild electron withdrawing groups make the insertion almost non regioselective; while strongly electron withdrawing groups are able to render secondary insertion favored. This trend indicates

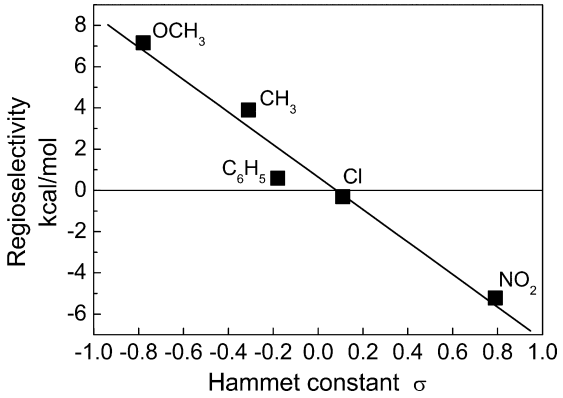

Fig. 4. Plot of the $\Delta E^{\neq}_{regio}$ vs. the Hammet parameter of the substituent on the C=C double bond, for insertion of different 1-alkenes into the Zr–Me bond of the **1Th-Zr** metallocene of Chart 1.

that the electronic property of the alkene might become an important factor in determining the regioselectivity of insertion.

The $\Delta E^{\neq}_{regio}$ we calculated for styrene and vinylchloride insertion into the Zr–Me bond of **1Th-Zr**, (0.60 and −0.30 kcal/mol, respectively), are quite small, which indicates that insertion is scarcely regioselective. The situation changes when a bulkier growing chain is considered. In fact, the $\Delta E^{\neq}_{regio}$ for styrene and vinylchloride insertion into the Zr–^{i}Pr bond of **1Th-Zr** are −1.7 and −0.8 kcal/mol, respectively, indicating that secondary insertion would be clearly favored on a secondary growing chain. This can be easily explained in light of the previous section results, which indicated that primary insertion is strongly disfavored on a secondary growing chain. Moreover, inversion of regiochemistry is also calculated if the $H_2Si <$ bridge is replaced by a $H_2C <$ bridge. In fact, the $\Delta E^{\neq}_{regio}$ we calculated for styrene insertion into the Zr–Me bond of $[H_2C(Cp_2)ZrMe]^{+}$ is −0.3 kcal/mol. In agreement with the experimental results [19], secondary insertion is favored in this case. This finding is related to the well known fact that the single-C bridge pulls down the two Cp rings of metallocenes. This creates a less crowded reactive pocket that can accommodate more easily a secondary inserting monomer.

3.1.5. CGC systems: role of the counterion

The final step of our analysis on the identification and evaluation of the factors influencing the regiochemistry of α-olefins insertion into a M–C bond is the role of the counterion. It is worthy to note that few theoretical studies [20], in agreement with many experimental studies [21], evidenced the remarkable role of the counterion in determining catalytic behavior and in particular on the activity of single-site group 4 metallocene and post-metallocene catalysts due to the ion-pairing phenomena. For these reasons, we calculated the 1,2 and 2,1 propene insertions for the **5Th-Ti** systems, in presence of the $[CH_3B(C_6F_5)_3]^{-}$ anion. The comparison of $\Delta E^{\neq}_{regio}$ computed for this system with and without counterion (see the values in Table 1 for **5Th-Ti** and **5Th-Ti + borate**) suggests that the counterion has negligible effect on the regiochemistry of this system. The optimized geometries of the two transition states are reported in Fig. 5. In agreement with the experimental results, our findings indicate that the regiochemical behavior of metallocenes is not influenced by the nature of the counterion [22].

3.2. Non-metallocene systems

In the previous section we rationalized the experimental and theoretical results obtained for the regiochemistry of propene insertion promoted by pseudo-tetrahedral precursors. In this section, we focus on the so-called non-metallocene systems with octahedral geometry of coordination. In the Introduction we pointed out that, contrarily to metallocenes and CGC systems, non-metallocene catalysts might promote both primary (e.g. phenoxy-amine Zr complexes, **2Oh**) or secondary propene propagation (e.g. phenoxy-imine Ti complexes, **1Oh**) with a regioselectivity strongly dependent of the ligand framework, as well as on the Group 4 metal involved. Here, we will discuss at the first the two paradigmatic examples **1Oh** and **2Oh**, further we will extend our analysis by ligand variation on "model" systems (systems **3**–**9Oh**) and, finally, we will show how the conclusions can be applied to "real catalysts" (systems **10**–**12Oh**) to easily rationalize the regiochemistry of propene insertion. All the mentioned systems are reported in Chart 1 whereas the results are summarized in Table 2.

3.2.1. Octahedral systems: ligand effect

The values reported in Table 2 show that the $\Delta E^{\neq}_{regio}$ calculated for the **1Oh-M** systems are roughly 2–3 kcal/mol lower than the corresponding **2Oh-M** ones. This indicates that the bis(phenoxy-amine) ligand "induces" primary propene insertion more effectively than the bis(phenoxy-imine) ligand. This seems an intrinsic feature of the ligands, since it is independent of the metal atom and of the growing chain.

In a recent paper we related the different regioselectivity of bis(phenoxy-amine) and bis(phenoxy-imine) catalysts to a balance of steric *and* electronic effects [11]. In particular,

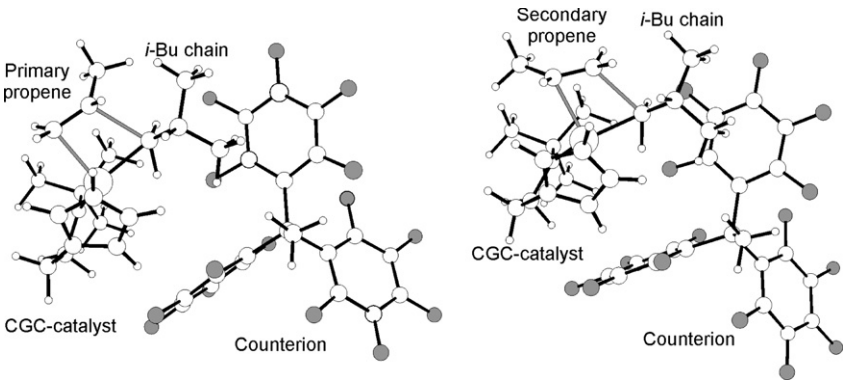

Fig. 5. Transition states for primary and secondary insertion into the Zr–^{i}Bu bond of the **5Th-Zr** CGC catalyst of Chart 1, in the presence of the $[CH_3B(C_6F_5)_3]^{-}$ counterion.

Table 2
Energy differences, in kcal/mol, between the transition states for 2,1 and 1,2 propene insertion ($\Delta E^{\ddagger}_{regio}$) for the octahedral systems reported in Chart 1

Model	Alkyl	$\Delta E^{\ddagger}_{regio}$	Model	Alkyl	$\Delta E^{\ddagger}_{regio}$
1Oh-Ti	Me	1.4	**5Oh-Ti**	Me	3.4
1Oh-Ti	^{i}Bu	0.2	**6Oh-Ti**	Me	2.1
1Oh-Ti	^{i}Pr	−2.9	**7Oh-Ti**	Me	3.3
1Oh-Zr	Me	2.2	**8Oh-Ti**	Me	4.1
1Oh-Hf	Me	2.4	**9Oh-Ti-1**	^{i}Bu	0.8
2Oh-Zr	Me	5.9	**9Oh-Ti-2**	^{i}Bu	0.1
2Oh-Zr	^{i}Bu	4.2	**10Oh-Ti**	^{i}Pr	−1.5
2Oh-Zr	^{i}Pr	1.1	**10Oh-Ti**	^{i}Bu	0.2 (3.5)[a]
2Oh-Ti	Me	4.6	**11Oh-Zr**	^{i}Bu	3.6 (5.2)[a]
3Oh-Ti	Me	1.3	**12Oh-Ti**	^{i}Bu	0.8
4Oh-Ti	Me	2.1			

[a] $\Delta E^{\neq}_{regio}$ of the "wrong" enantioface.

we found the existence, at the transition state, of an antibonding interaction between the MO corresponding to the incipient M–C bond and the MO corresponding to the lone pair of the N atom opposite to it. This *trans* influence is stronger for bis(phenoxy-amine) **2Oh** systems because the lone pair of the amine N atom is higher in energy (i.e. more electron-donating) than the corresponding lone pair of the imine N atom in the bis(phenoxy-imine) **1Oh** systems. Secondary propene insertion increases this destabilization due to the donating effect of the methyl group on the electron density of the incipient M–C bond. Since the presence of electronic effects might represent a challenging opportunity for a fine tuning of the regiochemistry insertion, we decided to investigate in more details this aspect.

In Fig. 6 we plot the $\Delta E^{\neq}_{regio}$ for propene insertion into the Ti–Me bond of systems **3Oh-9Oh** vs. the energy of the molecular orbital corresponding to the lone pair of the heteroatom trans to the incipient M–Me bond [23]. The plot of Fig. 6 shows an almost linear trend of the $\Delta E^{\neq}_{regio}$ vs. the basicity of the heteroatom, which supports

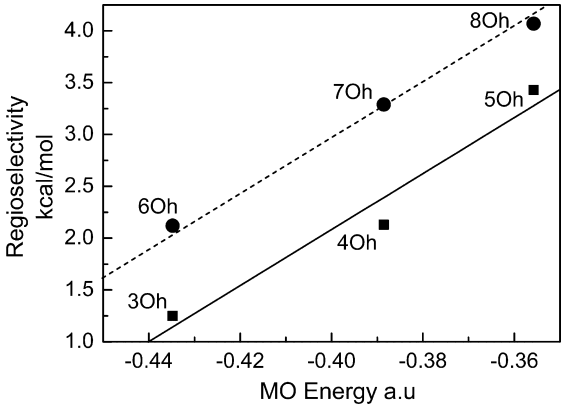

Fig. 6. $\Delta E^{\neq}_{regio}$ values reported as a function of the energy of the molecular orbital corresponding to the lone pair of the heteroatom trans to the monomer and to the growing chain for systems **3Oh-5Oh**, (squares) and systems **6Oh-8Oh** (circles) of Chart 1.

our preliminary hypothesis: more electron-donating atoms favor primary insertion while less electron-donating atoms favor secondary insertion. Finally, it is worthy to note that the $\Delta E^{\neq}_{regio}$ values for the systems with anionic S atoms (**6Oh-8Oh**) are about 1 kcal/mol higher than those calculated for the corresponding system with the anionic O atom (**3Oh-5Oh**).

Further support was obtained by the analysis of the C_1-symmetric model system **9Oh-Ti**, designed *ad hoc* with one active site having an amine N atom in trans to the chain (**9Oh-Ti-1**) and the other with an imine N atom in trans to the chain (**9Oh-Ti-2**). The two different $\Delta E^{\neq}_{regio}$ values reported in Table 2 are a good example of the variations in $\Delta E^{\neq}_{regio}$ by tuning the electronic properties of the ligand.

With these concepts in mind, it is simple to comment the values calculated for the "real systems **10Oh-Ti** [24a], **11Oh-Zr** and **12Oh-Ti** [25]. In fact, phenoxyketimine complexes show a slightly lower $\Delta E^{\neq}_{regio}$ compared to phenoxy-imine analogs (see **10Oh-Ti** and **1Oh-Ti**) [24b], and a similarly small change is calculated in the presence of a bulky ^{t}Bu group on the phenoxy-amine framework (compare **2Oh-Zr** with **11Oh-Zr**). A better preference for a primary propagation was calculated for the bis(phenolate) systems, **12Oh-Ti** compared to **10Oh-Ti** as expected by the plot reported in Fig. 6.

In conclusion, the main message that stems from this section is that the regiochemistry of propene insertion with octahedral systems can be finely tuned with a suitable choice of the electron properties of the heteroatoms coordinated to the metal. Ligands that increase electron density at the metal favor primary insertion, while ligands that make the metal more electron poor favor secondary insertion.

3.2.2. Octahedral systems: growing chain effect

Similarly to the case of the metallocene-based systems, (see Table 1), the $\Delta E^{\neq}_{regio}$ we calculated for propene insertion into M–^{i}Pr bond are always 2–3 kcal/mol lower then the $\Delta E^{\neq}_{regio}$ calculated for insertion into the M–^{i}Bu bond (see Table 2). In particular, when the growing chain is an isopropyl chain our calculations show an inversion of regioselectivity for propene insertion with the **1Oh-Ti** and **11Oh-Ti** system. This means that after a first 2,1 insertion, secondary propagation tends to be maintained because it does not require the formation of a sterically demanding head-to-head enchainment (see Fig. 7).

Differently, for the **2Oh-Zr** system propene insertion is predominantly 1,2. A secondary growing chain reduces this preference, but inversion of regioselectivity does not occur, in agreement with the experimental results [26].

3.2.3. Octahedral systems: metal effect

To investigate the effect of the metal atom, we compared the $\Delta E^{\neq}_{regio}$ for propene insertion into the M–^{i}Bu bond for the system **1Oh-M** with M = Ti, Zr, Hf. The $\Delta E^{\neq}_{regio}$ values vs. the ionic radius are reported in Fig. 8. The comparison of Figs. 3 and 8 shows that the two trends of $\Delta E^{\neq}_{regio}$ relative to the nature of the metals are opposite each other.

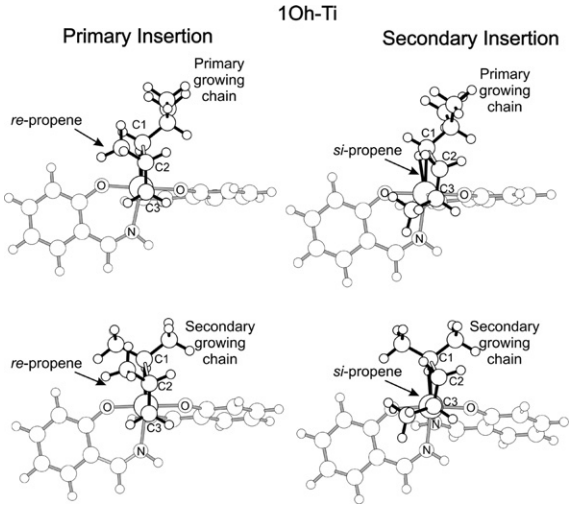

Fig. 7. Transition states for primary and secondary insertion into the M–^{i}Bu bonds (top) and M–^{i}Pr bonds (bottom) of the **1TOh-Ti** octahedral catalysts of Chart 1.

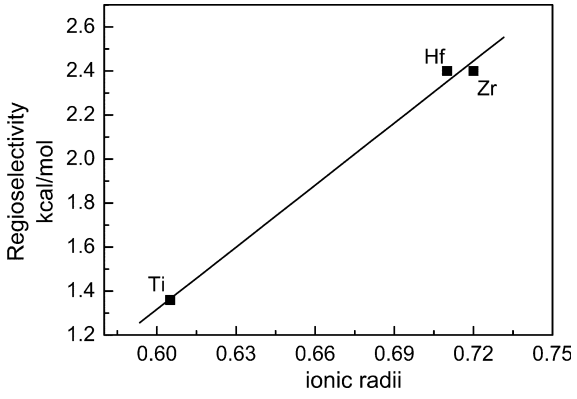

Fig. 8. Plot of the $\Delta E^{\neq}_{\text{regio}}$ vs. the ionic metal radius for propene insertion into the M–Me bond of the **1Oh-M** catalyst of Chart 1.

Since an increase of the ionic radius always produces an increase of the M–C distance and, consequently, a decrease of steric interactions between the secondary inserting monomer and the ligand framework, the trend reported in Fig. 8 indicates that the metal effect on the octahedral systems is not steric in nature. In particular, to a decrease of the metal acidity (Hf < Zr < Ti) corresponds an increase of the $\Delta E^{\neq}_{\text{regio}}$.

3.2.4. Octahedral systems: monomer effect

In this final section, we investigate the influence of the electronic structure of the monomer on regioselectivity. To this end, we calculate the $\Delta E^{\neq}_{\text{regio}}$ with different monomer by replacing the methyl group of propene with more or less electron-donating groups for **1Oh-Ti**–CH_3 system.

In Fig. 9 we report the trend of $\Delta E^{\neq}_{\text{regio}}$ as a function of the Hammet constant. Withdrawing groups such as NO_2 favor secondary insertion, whereas electron-donating groups cause the opposite effect. In agreement with previous hypothesis, electron donating groups destabilize the transition state for secondary monomer insertion by

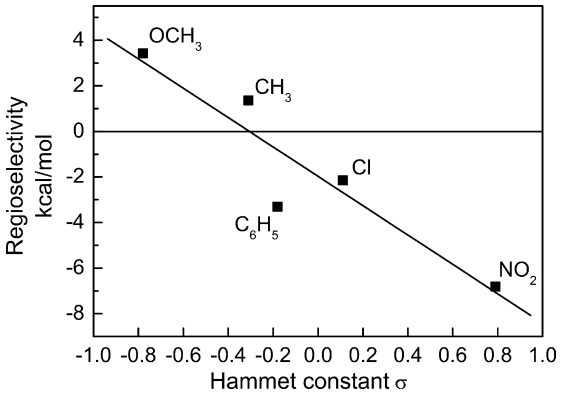

Fig. 9. Plot of the $\Delta E^{\neq}_{\text{regio}}$ vs. the Hammet parameter of the substituent on the C=C double bond, for insertion of different 1-alkenes into the Ti–Me bonds of the **1Oh** catalyst of Chart 1.

increasing the electron density on the secondary carbon atom, whereas withdrawing groups stabilize the transition state for secondary insertion. Comparing Figs. 4 and 9, we note that the effect due to variation of the electronic structure of the monomer is qualitatively the same in metallocene and octahedral systems, and in both cases the trend is almost linear, although the values of $\Delta E^{\neq}_{\text{regio}}$ for octahedral systems are lower than those calculated for metallocenes. In the case of **1Oh-Ti**–CH_3 inversion of regiochemistry from primary to secondary already occurs for styrene and vinyl chloride insertion, whereas for **1Th-Zr**–CH_3 inversion of regiochemistry toward 2,1 insertion was calculated only for a monomer with a very electron withdrawing NO_2 group ($\sigma = 0.78$).

4. Conclusions

In this paper we reported a systematic study of steric and electronic effects on the regiochemistry of 1-alkene insertion promoted by metallocene, constrained geometry and post-metallocene catalysts In particular we have analyzed the effects of ligand framework, growing chain, metal atoms, and different monomers. The main conclusions obtained are:

(i) In the case of metallocene and CGC based catalysts, the regiochemistry of monomer insertion is essentially dominated by steric effects because of the destabilization of the 2,1 transition state due to *steric* interaction between the incoming monomer and the ligand framework.

(ii) In the case of the octahedral systems, instead, the regiochemistry of monomer insertion is a balance between steric *and* electronic effects. In particular, electron-donating atoms coordinated trans to the inserting olefin stabilize the transition state for primary insertion.

(iii) Primary propene insertion on a secondary growing chain is disfavored by steric interactions between the methyl group of the propene and the growing

chain itself and such interaction strongly reduces the preference for primary insertion. For octahedral bis(phenoxy-imine) Ti based catalysts, primary propene insertion on a primary chain is only slightly favored, this implies that in the case of a secondary last inserted unit, secondary propene insertion is favored. Conversely, in the case of the bis(phenoxy-amine) based catalysts, primary insertion on a primary chain is strongly favored, and thus also in the case of propene insertion on a secondary last inserted unit, primary insertion is favored.

(iv) Finally, further support to an electronic effect on regiochemistry was obtained by examining monomers with different R groups. From a qualitative point of view, the monomer effect is the same for metallocenes and for octahedral systems. More electron-donating monomers favor primary insertion. However, this effect can have more practical consequences for octahedral systems than for metallocenes, since in the latter steric effects dominate.

The main message of this work is that regioselectivity of octahedral and metallocene systems has a different origin. For octahedral systems electronic effects seem to play an important role and it is possible to modulate the regiochemistry of 1-alkene insertion playing with the catalyst ligand framework.

Acknowledgements

This work was supported by INSTM (Cineca Grant Supercalcolo) and Basell Poliolefine Italia.

References

[1] P. Corradini, V. Busico, G. Guerra, in: G. Allen, J.C. Bevington (Eds.), Comprehensive Polymer Science, Pergamon Press, Oxford, 1988, p. 29.
[2] H.-H. Brintzinger, D. Fischer, R. Mülhaupt, B. Rieger, R.M. Waymouth, Angew. Chem., Int. Ed. 34 (1995) 1143.
[3] L. Resconi, L. Cavallo, A. Fait, F. Piemontesi, Chem. Rev. 100 (2000) 1253.
[4] A.L. McKnight, R.M. Waymouth, Chem. Rev. 98 (1998) 2587.
[5] E.Y. Tshuva, I. Goldberg, M. Kol, J. Am. Chem. Soc. 122 (2000) 10706.
[6] T.R. Boussie, G.M. Diamond, C. Goh, K.A. Hall, A.M. LaPointe, M.K. Leclerc, V. Murphy, J.A.W. Shoemaker, H. Turner, R.K. Rosen, J.C. Stevens, F. Alfano, V. Busico, R. Cipullo, G. Talarico, Angew. Chem., Int. Ed. 45 (2006) 3278.
[7] (a) A. Zambelli, I. Sessa, F. Grisi, R. Fusco, P. Accomazzi, Macromol. Rapid Commun. 22 (2001) 297;
(b) A. Zambelli, G. Allegra, Macromolecules 13 (1980) 42.
[8] (a) H. Makio, N. Kashiwa, T. Fujita, Adv. Synth. Catal. 344 (2002) 477;
(b) G.W. Coates, P.D. Hustad, S. Reinartz, Angew. Chem., Int. Ed. 41 (2002) 2236.
[9] C. De Rosa, F. Auriemma, M. Paolillo, L. Resconi, I. Camurati, Macromolecules 38 (2005) 9143.
[10] (a) G. Moscardi, L. Resconi, L. Cavallo, Organometallics 20 (2001) 1918–1931;
(b) P. Corradini, L. Cavallo, G. Guerra, in: J. Scheirs, W. Kaminsky (Eds.), Metallocene-Based Polyolefins: Preparation, Properties and Technology, Wiley, Chichester, 2000, p. 3;
(c) G. Guerra, P. Longo, L. Cavallo, P. Corradini, L. Resconi, J. Am. Chem. Soc. 119 (1997) 4394;
(d) G. Guerra, L. Cavallo, G. Moscardi, M. Vacatello, P. Corradini, J. Am. Chem. Soc. 116 (1994) 2988;
(e) M. Toto, L. Cavallo, P. Corradini, G. Moscardi, L. Resconi, G. Guerra, Macromolecules 31 (1998) 3431.
[11] G. Talarico, V. Busico, L. Cavallo, J. Am. Chem. Soc. 125 (2003) 7172.
[12] H. Kawamura-Kuribayashi, N. Koga, K. Morokuma, J. Am. Chem. Soc. 114 (1992) 8687.
[13] ADF 2005, Users Manual, Vrije Universiteit Amsterdam, Amsterdam, The Netherlands, 2005.
[14] (a) E.J. Baerends, D.E. Ellis, P. Ros, Chem. Phys. 2 (1973) 41;
(b) G. te Velde, E.J. Baerends, J. Comput. Phys. 99 (1992) 84.
[15] S.H. Vosko, L. Wilk, M. Nusair, Can. J. Phys. 58 (1980) 1200.
[16] A.D. Becke, Phys. Rev. A 38 (1988) 3098.
[17] (a) J.P. Perdew, Phys. Rev. B 33 (1986) 8822;
(b) J.P. Perdew, Phys. Rev. B 34 (1986) 7406.
[18] P. Corradini, G. Guerra, L. Cavallo, Acc. Chem. Res. 37 (2004) 231.
[19] L. Izzo, M. Napoli, L. Oliva, Macromolecules 36 (2003) 9340.
[20] (a) G. Lanza, I.L. Fragalà, T.J. Marks, Organometallics 21 (2002) 5594;
(b) G. Lanza, I.L. Fragalà, T.J. Marks, Organometallics 20 (2001) 4006;
(c) G. Lanza, I.L. Fragalà, T.J. Marks, J. Am. Chem. Soc. 122 (2000) 12764;
(d) Z. Xu, K. Vanka, T. Ziegler, Organometallics 23 (2004) 104;
(e) K. Vanka, Z. Xu, T. Ziegler, Can. J. Chem. 81 (2003) 1413;
(f) M.S.W. Chan, T. Ziegler, Organometallics 19 (2000) 5182.
[21] E.Y.-X. Chen, T.J. Marks, Chem. Rev. 100 (2000) 1391.
[22] (a) A. Rodriguez-Delgado, M.D. Hannant, S.J. Lancaster, M. Bochmann, Macromol. Chem. Phys. 205 (2004) 334;
(b) M. Bochmann, J. Organomet. Chem. 689 (2004) 3982.
[23] The molecular orbital energies of the lone pair were calculated with the package GAUSSIAN03 at MP2/6-31G++ level of theory. For each system a reduced model of the ligand (CH_2NH, CH_3NH_2 and CH_3SH for systems **3Oh-5Oh**, **4Oh-6Oh** and **5Oh-8Oh** of Chart 1, respectively) was considered.
[24] (a) A.F. Mason, G.W. Coates, J. Am. Chem. Soc. 126 (2004) 16326;
(b) From the experimental results of Ref. [24a], we can note that polypropylene NMR spectra produced by phenoxyketimine complexes **10Oh-Ti** show <5% of regioirregularities.
[25] C. Capacchione, A. Proto, H. Ebeling, R. Mülhaupt, K. Möller, T.P. Spaniol, J. Okuda, J. Am. Chem. Soc. 125 (2003) 4964.
[26] V. Busico, R. Cipullo, S. Ronca, P.H.M. Budzelaar, Macromol. Rapid Commun. 22 (2001) 1405.